Technical Report **1752**
August 1997

Frequency Dependencies of Target Highlights

G. A. Lengua

19971021 233

Approved for public release; distribution is unlimited.

Technical Report **1752**
August 1997

Frequency Dependencies of Target Highlights

G. A. Lengua

DTIC QUALITY INSPECTED 2

ADMINISTRATIVE INFORMATION

SB

EXECUTIVE SUMMARY

OBJECTIVE

The objective of this work was to examine the frequency dependencies of target highlights in order to determine where computational savings could be realized in broadband applications.

RESULTS

Significant savings can be achieved by simply separating all frequency independent calculations from the frequency loop. In some cases, highly accurate approximations will provide additional savings. In other cases, and contingent on the user's fidelity requirements, coarser approximations will yield yet more savings.

RECOMMENDATIONS

Separation of frequency-independent factors and accurate approximations should be implemented as soon as feasible. Coarser approximations should be implemented, but their use should be contingent on a tolerance test.

CONTENTS

Figures

INTRODUCTION

Accurate target models that predict submarine and surface ship echo time history are essential tools for antisubmarine warfare and ship vulnerability studies. A realistic model must account for the target's many highlights as well as insonification conditions. It must predict the highlight amplitude and phase as well as temporal and spectral behavior. These predictions require that researchers properly identify scattering mechanisms and incorporate them into the model.

Over the past 30 years, Naval Command, Control and Ocean Surveillance Center RDT&E Division (NRaD) researchers developed Uniform Theory of Diffraction (UTD) target models that provide an invaluable asset for torpedo signal-processing algorithms and torpedo-simulation development. NRaD has exported these models throughout the Navy. Previous NRaD target model formulations, dictated by past weapons' requirements and test scenarios, were monostatic, far field, and narrowband. They also used a simple Doppler implementation. These restrictions simplified the numerical implementation (as well as theoretical development) considerably. These models serve well in deep water and other benign environments. However, the littoral environment requires more sophistication.

A promising avenue for study involves broadband processing. Obviously simulation studies in this area require high-fidelity broadband target models. Practical considerations demand computational efficiency. This report examines the frequency dependencies of target highlights and determines how computational savings may be realized without undo loss of fidelity. The report first discusses general considerations followed by each highlight class, in turn.

GENERAL CONSIDERATIONS

Following Primakoff and Keller (1947), the scattering amplitude is taken to be the product of a geometrical factor, a phase-cancellation (directivity) factor, and a reflection factor. In addition, we include a loss factor to account for cover penetration.

GEOMETRICAL FACTOR

For a surface, the geometrical factor is

$$G = \frac{1}{2r\sqrt{1 + \dfrac{r}{R_A}}\sqrt{1 + \dfrac{r}{R_B}}},$$

where r is the range and R_A and R_B are the principal radii of curvature. For a line,

$$G = \frac{1}{r^{\frac{3}{2}}\sqrt{1 + \dfrac{2r\sin\psi}{R_A}}},$$

1

where ψ is the inclination angle. This factor is obviously independent of frequency.

PHASE-CANCELLATION FACTOR

The phase-cancellation factor is

$$P = P_H P_V$$

$$= \frac{1}{\sqrt{2}}\left[F\pm(\chi_{max}) - F\pm(\chi_{min})\right]\frac{1}{\sqrt{2}}\left[F\pm(\zeta_{max}) - F\pm(\zeta_{min})\right],$$

where

$$F_\pm(u) = \int_0^u e^{\pm i\frac{\pi}{2}\tau^2}\, d\tau$$

is the Fresnel integral and the arguments are

$$\chi_{max} = \sqrt{\frac{2}{\pi}k\left|\frac{1}{r} - \frac{2}{R_A}\right|}x_{max}$$

$$\chi_{min} = \sqrt{\frac{2}{\pi}k\left|\frac{1}{r} - \frac{2}{R_A}\right|}x_{min}$$

$$\zeta_{max} = \sqrt{\frac{2}{\pi}k\left|\frac{1}{r} - \frac{2}{R_B}\right|}z_{max}$$

$$\zeta_{min} = \sqrt{\frac{2}{\pi}k\left|\frac{1}{r} - \frac{2}{R_B}\right|}z_{min}$$

with k the wavenumber. Now,

$$F\pm(u) = C(u) \pm iS(u)$$

$$= \frac{1}{2}(1\pm i) - \left[g(u) \pm if(u)\right]e^{\pm i\frac{\pi}{2}u^2}$$

where $f(u)$ and $g(u)$ are auxiliary functions (Gautschi, 1965). These are odd functions and, for $0 \le u \le \infty$, have the rational approximations,

$$f(u) \approx \frac{1 + 0.926u}{2 + 1.792u + 3.104u^2}$$

$$g(u) \approx \frac{1}{2 + 4.142u + 3.492u^2 + 6.670u^3}.$$

2

Alternatively, series representations may be used (Boersma, 1960). Note that, if $\chi_{min} \approx -\chi_{max}$ and $\chi_{max} > 4$, $0.90 < |P_H| < 1.10$.

The case of a straight side must be treated separately. The observation point will be referenced to mid-height. Let h be the height of the side and γ the orientation angle with respect to the side. In the monostatic case, it can be shown (Chabries, 1975) that we may still use our earlier definition of P_V, but with

$$\zeta_{max} = \sqrt{\frac{2k}{\pi r}}\left(r\cos\gamma + \frac{1}{2}h\right)$$

and

$$\zeta_{min} = \sqrt{\frac{2k}{\pi r}}\left(r\cos\gamma - \frac{1}{2}h\right).$$

Alternatively, the results of Skudrzyk et al. (1973) may be used when $r \gg \dfrac{kh^2}{2\pi}$. Here they may be expressed as

$$P_V = \left[\sqrt{\frac{k}{\pi r}}he^{-i\frac{\pi}{4}}\right]\left[\frac{\sin(kh\cos\gamma)}{kh\cos\gamma}\right].$$

Note that the first term in brackets is the Sommerfeld–MacDonald factor for effecting the near field to far field transition (Ruck et al., 1970). The second term in brackets is the directivity of a line array. Note that for $kh\cos\gamma > 30$, P_V is usually insignificant.

REFLECTION AND TRANSMISSION COEFFICIENTS

Consider an acoustic wave in medium 3, a fluid (water), incident on medium 2, an elastic plate of thickness d, which in turn is backed by medium 1, a fluid (water or air). The reflection and transmission coefficients are given by Brekhovskikh (1980):

$$R = \frac{\left(M^2 - N^2\right)\dfrac{Z_1}{Z_3} + 1 + iM\left(1 - \dfrac{Z_1}{Z_3}\right)}{\left(M^2 - N^2\right)\dfrac{Z_1}{Z_3} - 1 - iM\left(1 + \dfrac{Z_1}{Z_3}\right)}$$

and

$$T = \frac{-2iN\dfrac{Z_1}{Z_3}\dfrac{\rho_3}{\rho_1}}{\left(M^2 - N^2\right)\dfrac{Z_1}{Z_3} - 1 - iM\left(1 + \dfrac{Z_1}{Z_3}\right)},$$

3

where

$$M = \frac{Z_{2C}}{Z_3}\cos^2\left(2\theta_{2S}\right)\cot P + \frac{Z_{2S}}{Z_3}\sin^2\left(2\theta_{2S}\right)\cot Q,$$

$$N = \frac{Z_{2C}}{Z_3}\frac{\cos^2\left(2\theta_{2S}\right)}{\sin P} + \frac{Z_{2S}}{Z_3}\frac{\sin^2\left(2\theta_{2S}\right)}{\sin Q},$$

$$P = k_{2C}d\cos\theta_{2C},$$

$$Q = k_{2S}d\cos\theta_{2S},$$

$$Z_1 = \frac{\rho_1 c_1}{\cos\theta_1},$$

$$Z_{2C} = \frac{\rho_2 c_{2C}}{\cos\theta_{2C}},$$

$$Z_{2S} = \frac{\rho_2 c_{2S}}{\cos\theta_{2S}},$$

$$Z_3 = \frac{\rho_3 c_3}{\cos\theta_3},$$

$$c_{2C}^2 = \frac{E_2}{\rho_2\left(1-\sigma_2^2\right)},$$

$$c_{2S}^2 = \frac{G_2}{\rho_2},$$

and

$$G_2 = \frac{E_2}{2\left(1+\sigma_2\right)}.$$

The propagation angles (measured from the normal) are related by Snell's law,

$$k_3\sin\theta_3 = k_{2C}\sin\theta_{2C} = k_{2S}\sin\theta_{2S} = k_1\sin\theta_1.$$

Typical values for steel are $\rho = 7.8\times 10^3\ \frac{\text{kg}}{\text{m}^3}$, $E = 2.17\times 10^{11}\ \frac{\text{N}}{\text{m}^2}$, and $\sigma = 0.284$. Hence,

$c_C = 5501\ \frac{\text{m}}{\text{s}}$ and $c_S = 3291\ \frac{\text{m}}{\text{s}}$.

Monostatic Reflection Factor

In the monostatic case, $\theta_3 = 0$ and, consequently, all the other propagation angles are zero as well. Here,

$$R_M = \frac{-\left(\dfrac{Z_{2C}}{Z_3}\right)^2 \dfrac{Z_1}{Z_3} + 1 + i\left(1 - \dfrac{Z_1}{Z_3}\right)\dfrac{Z_{2C}}{Z_3}\cot P_M}{-\left(\dfrac{Z_{2C}}{Z_3}\right)^2 \dfrac{Z_1}{Z_3} - 1 - i\left(1 + \dfrac{Z_1}{Z_3}\right)\dfrac{Z_{2C}}{Z_3}\cot P_M}$$

with $P_M = k_{2C}d$. Then,

$$|R_M|^2 = \frac{\left[1 - \left(\dfrac{Z_{2C}}{Z_3}\right)^2 \dfrac{Z_1}{Z_3}\right]^2 + \left(1 - \dfrac{Z_1}{Z_3}\right)^2\left(\dfrac{Z_{2C}}{Z_3}\right)^2 \cot^2 P_M}{\left[1 + \left(\dfrac{Z_{2C}}{Z_3}\right)^2 \dfrac{Z_1}{Z_3}\right]^2 + \left(1 + \dfrac{Z_1}{Z_3}\right)^2\left(\dfrac{Z_{2C}}{Z_3}\right)^2 \cot^2 P_M}.$$

The extrema are found from the requirement $\dfrac{d|R_M|}{dP_M} = 0$ to be given by the conditions $\cos P_M = 0$ and $\sin P_M = 0$. Correspondence with maxima and minima depends on the impedances. Hence,

$$\left|R_{M,\text{ext1}}\right| = \frac{\left|1 - \left(\dfrac{Z_{2C}}{Z_3}\right)^2 \dfrac{Z_1}{Z_3}\right|}{\left|1 + \left(\dfrac{Z_{2C}}{Z_3}\right)^2 \dfrac{Z_1}{Z_3}\right|}$$

and

$$\left|R_{M,\text{ext2}}\right| = \frac{\left|1 - \dfrac{Z_1}{Z_3}\right|}{\left|1 + \dfrac{Z_1}{Z_3}\right|}.$$

It is useful to note some impedance values: $Z_{\text{water}} = 1.5 \times 10^6 \ \dfrac{\text{kg}}{\text{m}^2\text{s}}$, $Z_{\text{air}} = 4.1 \times 10^2 \ \dfrac{\text{kg}}{\text{m}^2\text{s}}$, and $Z_{C,\text{steel}} = 4.3 \times 10^7 \ \dfrac{\text{kg}}{\text{m}^2\text{s}}$. Therefore, a water-backed plate has $\left|R_{M,\text{min}}\right| = 0$ and $\left|R_{M,\text{max}}\right| = 0.9976$, while an air-backed plate has $\left|R_{M,\text{min}}\right| = 0.6332$ and $\left|R_{M,\text{max}}\right| = 0.9995$. For a 2.5-cm-thick plate, the minima and maxima are separated by 55 kHz.

Loss Factor

Since the penetration angle can range between 0 and very close to $\dfrac{\pi}{2}$, no simplifications can be made to the transmission coefficient.

HULLS

Since the specular point search and principal curvature calculations are independent of frequency, they should be clearly separated from the remaining calculations.

SAILS AND CONTROL PLANES

Since the specular point search and principal curvature calculations are independent of frequency, they should be clearly separated from the remaining calculations.

EDGES AND WEDGES

We will use cylindrical coordinates (ρ, ϕ, z). The wedge surfaces will be defined as $\phi = 0$ and $\phi = 2\pi - \phi_{\text{Wedge}}$. Let ν be defined as

$$\nu\pi = 2\pi - \phi_{\text{Wedge}}.$$

Note that an edge has $\nu = 2$. For plane wave scattering from a straight wedge, Pauli (1938) gives the monostatic solution:

$$\Phi_{\text{Pauli}} = v_B(\phi) + v_B(0),$$

where

$$v_B(\psi) = \frac{e^{i\frac{\pi}{4}}}{2\sqrt{\pi}}\left[\frac{2}{\nu}\sin\frac{\pi}{\nu}\right]\left[\frac{2\cos\dfrac{\psi}{2}}{\cos\dfrac{\pi}{\nu} - \cos\dfrac{\psi}{\nu}} e^{ik\rho\cos\psi} F^{\text{com}}\left(\sqrt{k\rho(1+\cos\psi)}\right) + \cdots\right]$$

and

$$F^{\text{com}}(z) = \int_z^\infty e^{-i\tau^2}\,d\tau$$

is the complementary Fresnel integral. $F^{\text{com}}(z) = \sqrt{\dfrac{\pi}{2}}E_1^{\text{com}}(z)$ of Abramowitz and Stegun (1965).

For a straight wedge of length, h, and scattering of a spherical wave, the solution is

$$\Phi = \frac{\sin^2 \gamma}{r} \sqrt{\frac{\rho}{2r}} P_V \Phi_{\text{Pauli}},$$

where γ is the angle with respect to the edge and P_V was discussed in the Phase-Cancellation Factor section.

HULL INTERNALS

The problem here is in the determination of the transmission coefficients. Since the penetration angle calculations are independent of frequency, they should be clearly separated from the remaining calculations.

SAIL INTERNALS

The problem here is in the determination of the transmission coefficients. Since the penetration angle calculations are independent of frequency, they should be clearly separated from the remaining calculations.

PROPELLERS

The hydrofoil formulation of Lengua (1991) is used. Since the specular point search and principal curvature calculations are independent of frequency, they should be clearly separated from the remaining calculations.

PROPELLER CAPS

Consider a plane wave, of wavenumber, k, incident upon a finite cone with a flat base. Denote the half-angle of the cone by γ and the radius of the base by a. The height is then $h = a \cot \gamma$. Polar coordinates (r, ϕ) are used, with the origin at the tip of the cone. The values $\phi = 0$ and $\phi = \pi$ represent axial incidence upon the tip and base, respectively. For the purposes of this discussion, the base is always shadowed. Thus, only the interval, $0 \le \phi \le \frac{\pi}{2}$, will be considered. When $\phi = \frac{\pi}{2} - \gamma$ (broadside), there is specular reflection from the surface of the cone.

It is useful to examine the problem from a geometrical theory of diffraction perspective. First note that, for $0 < \phi < \gamma$, two singly diffracted rays from the edge are returned to the source. Hence, the backscattered field is an oscillatory function of ka, due to interference between these rays. For $\gamma < \phi < \frac{\pi}{2}$, only one singly diffracted ray from the edge is returned to the source. Hence, the field does not oscillate as a function of ka. Also note that for $\phi = 0$, the edge diffracted rays have an

axial caustic.

For a unit amplitude incident field, the scattered field is

$$p(r,\phi) = \frac{e^{ikr}}{kr} D(\phi) ,$$

where D is the diffraction coefficient. Kouyoumjian (1977) has determined uniform solutions through the axis and broadside. Let

$$n = \frac{3}{2} + \frac{\gamma}{\pi} .$$

Then, for $0 \le \phi < \gamma$,

$$D(\phi) = ka \frac{\sin\frac{\pi}{n}}{n} J_0(2ka\sin\phi)e^{i2ka\cot\gamma}\left[\frac{1}{\cos\frac{\pi}{n}-1} \pm \frac{1}{\cos\frac{\pi}{n}-\cos\frac{3\pi}{n}}\right] ,$$

where J_0 is the zero-order Bessel function and the upper (lower) sign applies to the hard (soft) case. For $\gamma < \phi \le \frac{\pi}{2}$,

$$D(\phi) = \frac{1}{4}\sqrt{\frac{ka}{\pi\sin\phi}}e^{-i\left[2ka\csc\gamma\cos(\gamma+\phi)+\frac{\pi}{4}\right]}\tan(\gamma+\phi)\Gamma\left[2ka\csc\gamma\cos(\gamma+\phi)\right] ,$$

where

$$\Gamma(x) = \begin{cases} 1 - \frac{1}{2}e^{i\left(x-\frac{\pi}{4}\right)}\sqrt{\frac{\pi}{x}} + \frac{F(x)}{2ix} & \text{for } x>0 \\ 1 - \frac{1}{2}e^{i\left(x+\frac{\pi}{4}\right)}\sqrt{\frac{\pi}{|x|}} + \frac{F^*(|x|)}{2ix} & \text{for } x<0 \end{cases}$$

with

$$F(z) = 2i\sqrt{|z|}e^{iz}\int_{\sqrt{|z|}}^{\infty}e^{-i\tau^2}\,d\tau .$$

Now, for $|z| \ll 1$, $F(z) \approx e^{i\left(z+\frac{\pi}{4}\right)}\left[\sqrt{\pi z} - 2ze^{i\frac{\pi}{4}} - \frac{2}{3}z^2 e^{-i\frac{\pi}{4}}+\cdots\right]$ and, consequently, for $|x| \ll 1$,

$\Gamma(x) \approx -i\frac{2}{3}x$. Thus, at broadside,

$$D\left(\frac{\pi}{2}-\gamma\right) = \sqrt{\frac{(ka)^3}{9\pi\sin^2\gamma\cos\gamma}}e^{i\frac{5\pi}{4}} .$$

For $|z| \gg 1$, $F(z) \approx 1 + \dfrac{1}{2} i \dfrac{1}{z} - \dfrac{3}{4} \dfrac{1}{z^2} + \cdots$ and, consequently, for $|x| \gg 1$,

$\Gamma(x) \approx 1 - \dfrac{1}{2} e^{i\left(x - \frac{\pi}{4}\right)} \sqrt{\dfrac{\pi}{x}} - \dfrac{1}{2} i \dfrac{1}{x}$. This is typically a good approximation to within a few degrees of broadside.

Note that there is a discontinuity at $\phi = \gamma$. The transition about this region is extremely difficult to formulate. However, the scattering amplitude there is typically so small as to not be a concern.

CORNERS

Let us consider a dihedral corner, represented as a flange on a cylinder. It is useful to first discuss the special case of a plane wave, of wavenumber, k, and unit amplitude, incident upon a finite cylinder, of radius, a, and length, $2d$, at whose center is a flange, of height, h, and at a right angle to the cylinder. Let θ denote the angle of incidence with respect to the cylinder normal. The scattering amplitude depends on the extent of the wave reflected from the corner back to the source, or "aperture" of the corner. Now, monostatic reflection from the cylinder and flange is equivalent to bistatic reflection from the cylinder to the virtual image of the source. The flange acts as the plane of reflection. If the cylinder were of infinite length, the aperture would be $L = 2h \tan \theta$. For a finite cylinder, the aperture is limited to its length. Thus,

$$L = 2 \min[d, h \tan \theta].$$

Bistatic reflection from a cylinder of length, L, has the amplitude,

$$P_{\text{Basic}} = \sqrt{\dfrac{ka \cos \theta}{4\pi}} L,$$

assuming $ka \cos \theta \gg 1$.

For a spherical wave, from a source at a range, $r \gg 2d$, the backscattering amplitude is

$$P = \dfrac{P_{\text{Basic}}}{r^2}.$$

Let us now consider the general case. Let the corner have an angle $\dfrac{\pi}{2} + \phi$ and an aperture covering the interval, $x_1 \leq x \leq x_2$. Then, it can be shown (Sides, 1976) that the backscattering amplitude is multiplied by a correction factor,

$$B = \dfrac{r^2}{kL} \sum_{n=0}^{N} A_n e^{i\Gamma_n},$$

9

where

$$A_n = \frac{\sqrt{\cos(\phi + \beta_n)} \, \sin\left[k\Delta x \sin(\phi + \beta_n)\right]}{r_n^2 \sin(\phi + \beta_n)}$$

$$\Gamma_n = -2k(r_n - r)$$

$$\beta_n = \arctan\left[\frac{\dfrac{x_n}{r_n}\cos\phi}{\sqrt{1 - \left(\dfrac{x_n}{r_n}\cos\phi\right)^2}}\right]$$

and

$$r_n^2 = r^2 + x_n^2 + 2rx_n \sin\phi,$$

with $x_n = x_1 + n\Delta x$ and $N = \dfrac{L}{\Delta x}$. A typical increment is $\Delta x = \dfrac{1}{2k}$.

In the continuum limit,

$$B = \frac{r^2}{L} \int_{x_1}^{x_2} \frac{\sqrt{\cos\left[\phi + \arctan\left(\dfrac{x\cos\phi}{r + x\sin\phi}\right)\right]}}{r^2 + x^2 + 2rx\sin\phi} e^{-2ik\left[\sqrt{r^2 + x^2 + 2rx\sin\phi} - r\right]} dx,$$

which cannot be evaluated analytically, the summation expression is more suited for numerical calculation. However, if $r \to \infty$,

$$B \to \sqrt{\cos\phi} \, \frac{\sin(kL\sin\phi)}{kL\sin\phi} e^{-2ik\frac{x_1 + x_2}{2}\sin\phi}.$$

Note that this is the product of three terms. The first may be considered an obliquity factor. The second is the directivity of a line array. Hence, a non-right corner is analogous to non-normal incidence. The third term represents a shift of the phase center.

When $r \gg |x_{1,2}|$,

$$B \approx \sqrt{\frac{\pi r\cos\phi}{2kL^2}} \left\{ F_\pm\left[\sqrt{\frac{2k}{\pi r}}(r\sin\phi + x_2)\right] - F_\pm\left[\sqrt{\frac{2k}{\pi r}}(r\sin\phi + x_1)\right] \right\} e^{ikr\sin^2\phi}.$$

This is usually a satisfactory approximation.

TANKS

Tanks can be very complex physical structures and very difficult to model in detail. They do not wrap completely around the hull but are separated by longitudinal plates. They may be reinforced with ribs and/or stringers. Some may contain air flasks. They contain fluids of various types and may hold a combination of sea water and air.

To allow analysis, a number of simplifying assumptions are made. The separator plates, stringers, and flasks are not modeled. Therefore, only dihedral corners are considered. Each tank is uniformly filled with a specified fluid. A tank is taken to be formed by concentric hulls bounded by deep frames.

Multiple reflections (bounces) within a tank are designated by a pair of integers, $[N, M]$, following the notation of Sides (1976). N refers to the number of times a ray is reflected from bulkheads. M refers to the number of times a ray is reflected by hulls.

For the case of plane-wave incidence and right-angle corners, the backscattering amplitude of an $[N, M]$ bounce is

$$A_{\text{Basic}} = R_{\text{B1}}^{N-1} R_{\text{B2}}^{N} R_{\text{OH}}^{M-1} R_{\text{PH}}^{M} \sqrt{\frac{ka \cos \theta}{4\pi}} [T_1 d_1 + T_2 d_2] \ .$$

This is composed of several factors. The square-root term is the amplitude of an ideal corner reflector, as discussed in the previous section. There is a reflection coefficient, R, for each wall of the tank. The factor in brackets consists of "transmission windows" of length, d_1 and d_2, multiplied by the transmission factors, T_1 and T_2. Since rays must pass through either the leading bulkhead, outer hull, or both, the appropriate factors must be used. In terms of the transmission coefficients, the three possibilities are T_{B1}^{2}, T_{OH}^{2}, or $T_{\text{B1}} T_{\text{OH}}$. Therefore, d must be divided into regions of constant transmission factor.

The general case includes a correction factor as discussed in the previous section on corners.

One possible way to account for the effects of clutter is through a mean free path approach. This is obviously a stochastic analysis, so agreement is only expected in the aggregate and not for particular realizations. The mean free path, Λ, may be inferred from schematics or experimental data. The amplitude of a particular bounce is then reduced by a factor, $e^{-d/\Lambda}$.

It is readily apparent that because of the reflection and transmission coefficients, the frequency dependence is a complicated function. Experience shows that higher order bounce numbers do not make an appreciable contribution, so that the tank response may be simply taken as the $[1,1]$ bounce. At this level of approximation, R_{PH} may be taken as unity.

FRAMES

The problem of scattering from hull stiffeners is very complex and has been the subject of considerable debate. We use the Hayek and Karali (1993) and Hayek (1997) formulation. Consider

a plane wave of amplitude, Φ_0, incident at an angle, θ_0, with respect to the normal, on an elastic plate of thickness, h. Let ρ, D, and G be the density, flexural rigidity, and shear modulus of the plate, respectively, and let $\kappa^2 = \pi^2 \big/ 12$. Let

$$D = \frac{Eh^3}{12(1-v^2)}$$

$$G = \frac{E}{2(1+v)},$$

with E and v the Young's modulus and Poisson's ratio of the plate.

The reflection coefficient of an infinite plate without discontinuities and with fluid loading on one side only is given by

$$V(\theta_0) = -\frac{a(\theta_0) - ib(\theta_0)}{a(\theta_0) + ib(\theta_0)},$$

where

$$a(\theta_0) = F_5 + F_3 \sin^2 \theta_0$$

$$b(\theta_0) = \left[\sin^4 \theta_0 - F_1 \sin^2 \theta_0 + F_2 \right] \cos \theta_0 .$$

Here,

$$F_1 = \frac{\rho \omega^2}{k_0^2} \left[\frac{1}{\kappa^2 G} + \frac{h^3}{12D} \right] = \left[\frac{24}{\pi^2} \frac{1}{1-v} + 1 \right] \left(\frac{c_p}{c_0} \right)^{-2}$$

$$F_2 = \frac{\rho h \omega^2}{k_0^4} \left[\frac{\rho h^2 \omega^2}{12 \kappa^2 GD} - \frac{1}{D} \right] = \frac{24}{\pi^2} \frac{1}{1-v} \left(\frac{c_p}{c_0} \right)^{-4} - \frac{1}{\Omega^2}$$

$$F_3 = \frac{\rho_0 \omega^2}{k_0^3} \frac{1}{\kappa^2 Gh} = \frac{4\sqrt{3}}{\pi^2} \frac{\rho_0}{\rho} \frac{1}{1-v} \left(\frac{c_p}{c_0} \right)^{-1} \frac{1}{\Omega}$$

$$F_5 = \frac{\rho_0 \omega^2}{k_0^5} \left[\frac{1}{D} - \frac{\rho h^2 \omega^2}{12 \kappa^2 GD} \right] = \left[-\frac{4\sqrt{3}}{\pi^2} \frac{1}{1-v} \left(\frac{c_p}{c_0} \right)^{-3} + \frac{1}{2\sqrt{3}} \frac{c_p}{c_0} \frac{1}{\Omega^2} \right] \frac{\rho_0}{\rho} \frac{1}{\Omega}$$

and we also define

$$F_6 = \frac{\rho_0 \omega^2}{k_0^5} \frac{1}{D} = \frac{1}{2\sqrt{3}} \frac{c_p}{c_0} \frac{\rho_0}{\rho} \frac{1}{\Omega^3} .$$

The thin-plate speed,

$$c_p = \sqrt{\frac{E}{\rho\left(1 - v^2\right)}}$$

and $\Omega = \dfrac{\omega}{\omega_c}$, where the critical frequency is

$$\omega_c = \frac{\sqrt{12}c_0^2}{hc_p}.$$

The result for the scattered field is, after a steepest descent approximation,

$$\Psi \approx \Phi_0\left[1 - V(\theta_0)\right]\frac{\exp\left[i\left(k_0 r - \frac{\pi}{4}\right)\right]}{\sqrt{k_0 r}}\cos\theta\frac{C_0 + C_1\sin\theta + C_2\sin^2\theta}{F_5 + F_3\sin^2\theta + i\cos\theta\left[\sin^4\theta - F_1\sin^2\theta + F_2\right]}$$

$$\pm 2\pi i\sum \text{residues [between S and L]},$$

where θ is the observation angle and the residues in this expression are from the poles enclosed between the steepest descent path and the original path of integration. The $\pm$ sign is due to the fact that the two paths cross one another. Hence, the sign depends on where the pole is located, that is, whether it is encircled clockwise or counterclockwise. The residues may be calculated as

$$\text{residue of } \alpha_j = \Phi_0\left[1 - V(\theta_0)\right]\exp\left[ik_0 r\cos(\alpha - \theta)\right]\cos\alpha\frac{C_0 + C_1\sin\alpha + C_2\sin^2\alpha}{\dfrac{d}{d\alpha}Q(\sin\alpha)}\Bigg|_{\alpha=\alpha_j},$$

where $Q\left(\sin\alpha_j\right) = 0$, with

$$Q(\lambda) = F_5 + F_3\lambda^2 + \sqrt{\lambda^2 - 1}\left[\lambda^4 - F_1\lambda^2 + F_2\right],$$

and

$$\frac{d}{d\alpha}Q(\sin\alpha) = 2F_3\sin\alpha\cos\alpha + i\sin\alpha\left[-F_2 + F_1\left(\sin^2\alpha - 2\cos^2\alpha\right) - \sin^4\alpha + 4\sin^2\alpha\cos^2\alpha\right].$$

The result is only valid for large $k_0 r$, and it fails near grazing because $\cos\theta \to 0$. The coefficients, C_n, are given by

$$C_0 = \frac{\sqrt{2\pi}iZ_f k_0^2 F_5}{2\pi i\omega\rho_0 - Z_f k_0^2 F_5 I_0 - Z_f k_0^2 F_3 I_2}\cos\theta_0$$

$$C_1 = \frac{\sqrt{2\pi i} Z_m k_0^4 F_6}{2\pi i \omega \rho_0 + Z_m k_0^4 F_6 I_2} \sin\theta_0 \cos\theta_0$$

$$C_2 = \frac{\sqrt{2\pi i} Z_f k_0^2 F_3}{2\pi i \omega \rho_0 - Z_f k_0^2 F_5 I_0 - Z_f k_0^2 F_3 I_2} \cos\theta_0 ,$$

where

$$I_n = \int_{-\infty}^{\infty} \frac{\lambda^n \sqrt{\lambda^2 - 1}}{Q(\lambda)} d\lambda .$$

Z_f and Z_m are the line force and moment impedances, respectively, of the frame.

It is obvious that this has an extremely complicated frequency dependence before even considering the dependencies of Z_f and Z_m. There is no satisfactory way to approximate these results over any appreciable frequency range. However, it is possible to achieve significant computational savings.

APPROXIMATIONS TO INTEGRALS

Calculation of the I_n via numerical integration involves considerable computation time. For high frequencies they may be approximated. The procedure is as follows. Write

$$Q(\lambda) = \sqrt{\lambda^2 - 1}\left[\lambda^4 - \lambda_1^2\right]\left[\lambda^4 - \lambda_2^2\right] + F_5 + F_3\lambda^2 ,$$

where

$$\lambda_{1,2}^2 = \frac{1}{2}\left\{ F_1 \pm \sqrt{F_1^2 - 4F_2} \right\} .$$

Note that for $\Omega \gg 1$, the F_3 and F_5 terms are small. Also note that for most materials, $F_1 \gg F_2$ (and $F_3 \gg F_5$). Hence, the integral is dominated by the regions about $\lambda^2 = \lambda_2^2$. The approximation consists of using this value of λ within the radical, so that

$$I_n \approx \int_{-\infty}^{\infty} \frac{\lambda^n d\lambda}{\lambda^4 - \left(F_1 + i\dfrac{F_3}{\sqrt{1 - \lambda_2^2}} \right)\lambda^2 + F_2 - i\dfrac{F_5}{\sqrt{1 - \lambda_2^2}}} .$$

Observe that for odd n, $I_n = 0$. Let $\lambda = \sqrt{x}$, then for even n,

$$I_n \approx \int_0^{\infty} \frac{x^{\frac{1}{2}n - \frac{1}{2}} dx}{(x - z_1)(x - z_2)} ,$$

14

where

$$z_{1,2} = \frac{1}{2}\left\{ F_1 + i\frac{F_3}{\sqrt{1-\lambda_2^{\,2}}} \pm \sqrt{\left(F_1 + i\frac{F_3}{\sqrt{1-\lambda_2^{\,2}}} \right)^2 - 4\left(F_2 - i\frac{F_5}{\sqrt{1-\lambda_2^{\,2}}} \right)} \right\}.$$

Now,

$$\int_0^\infty \frac{x^{\mu-1}\,dx}{(x+\beta)(x+\gamma)} = \frac{\pi}{\gamma-\beta}\left[\beta^{\mu-1} - \gamma^{\mu-1}\right]\csc(\mu\pi)$$

for $|\arg\beta| < \pi$, $|\arg\gamma| < \pi$, and $0 < \operatorname{Re}\mu < 2$ (Gradshteyn, 1980). Thus,

$$I_n \approx \frac{\pi}{z_1 - z_2}\left[(-z_1)^{\frac{1}{2}(n-1)} - (-z_2)^{\frac{1}{2}(n-1)}\right]\csc\left[(n+1)\frac{\pi}{2}\right].$$

Specifically, we have

$$I_0 \approx -\frac{i\pi}{z_1 - z_2}\left[\frac{1}{\sqrt{z_2}} - \frac{1}{\sqrt{z_1}}\right]$$

and

$$I_2 \approx -\frac{i\pi}{z_1 - z_2}\left[\sqrt{z_1} - \sqrt{z_2}\right].$$

Let us consider a 5-cm-thick steel plate (coincidence frequency of 4.7 kHz). The "exact" and approximate results are compared in figures 1 and 2. As can be seen, the general behavior is followed, but not the oscillations. This is not as serious a problem as might first be expected, because their effect is mitigated by the manner in which they enter the C_n. Figures 3 through 11 compare the results for the non-angular parts of C_0, C_1, and C_2 for three cases. Case 1 has

$Z_f = 10^3 i\,\dfrac{\text{N-s}}{\text{m}^2}$ and $Z_m = 10^3 i\,\text{N-s}$. Case 2 has $Z_f = 10^6 i\,\dfrac{\text{N-s}}{\text{m}^2}$ and $Z_m = 10^3 i\,\text{N-s}$. Case 3 has

$Z_f = 10^3 i\,\dfrac{\text{N-s}}{\text{m}^2}$ and $Z_m = 10^6 i\,\text{N-s}$. Some general observations may be made, based on cases ran

between the ones presented. C_0 shows good agreement for $\Omega > 1$ in all cases. C_1 shows the general behavior, but not the oscillations. Errors will be less than 3 dB for $\Omega > 2$, except when $|Z_m| > 10^5$. C_2 shows good agreement for $\Omega > 6$ in all cases. It shows good agreement for $\Omega > 2$, except when $|Z_f| > 10^5$.
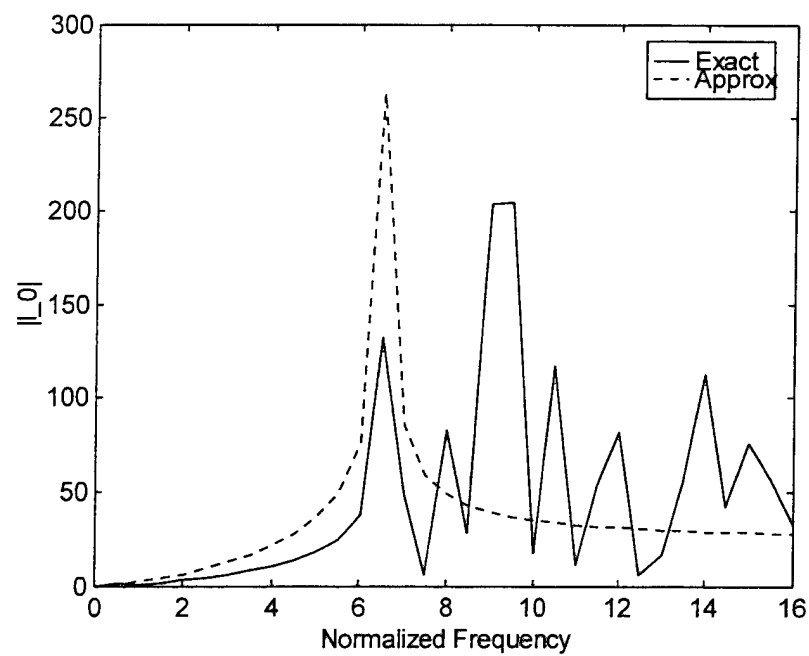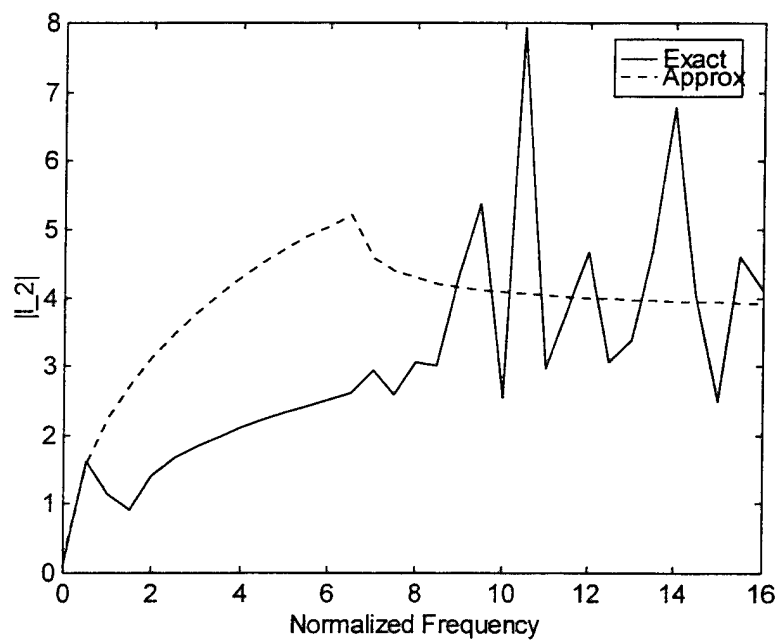
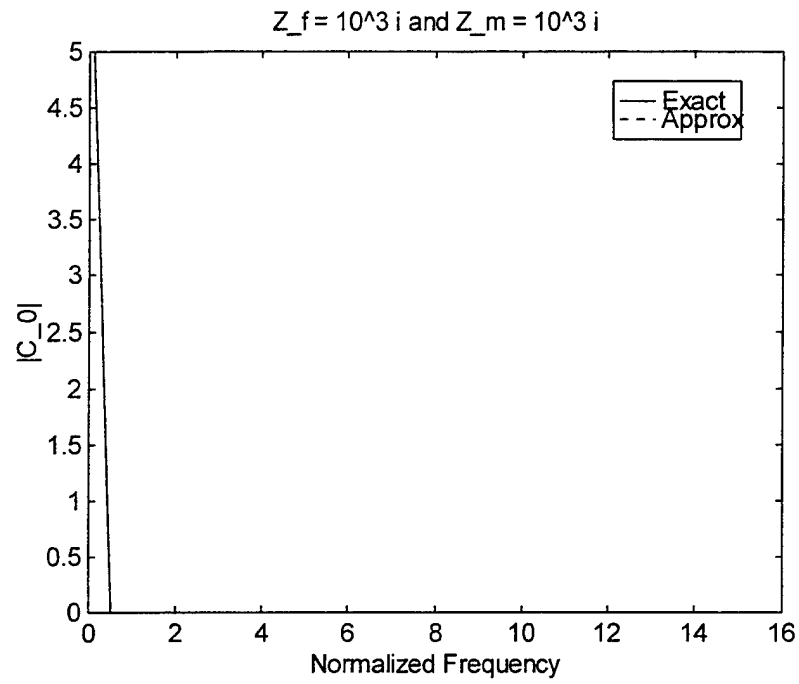Figure 1. Comparison for I_0.

Figure 2. Comparison for I_2.

Figure 3. Comparison for non-angular part of C_0 : Case 1
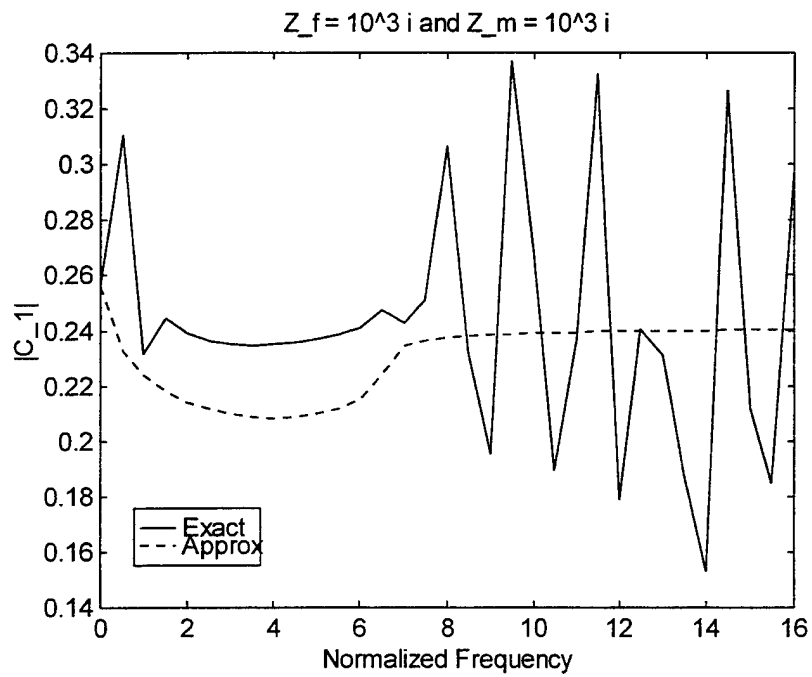

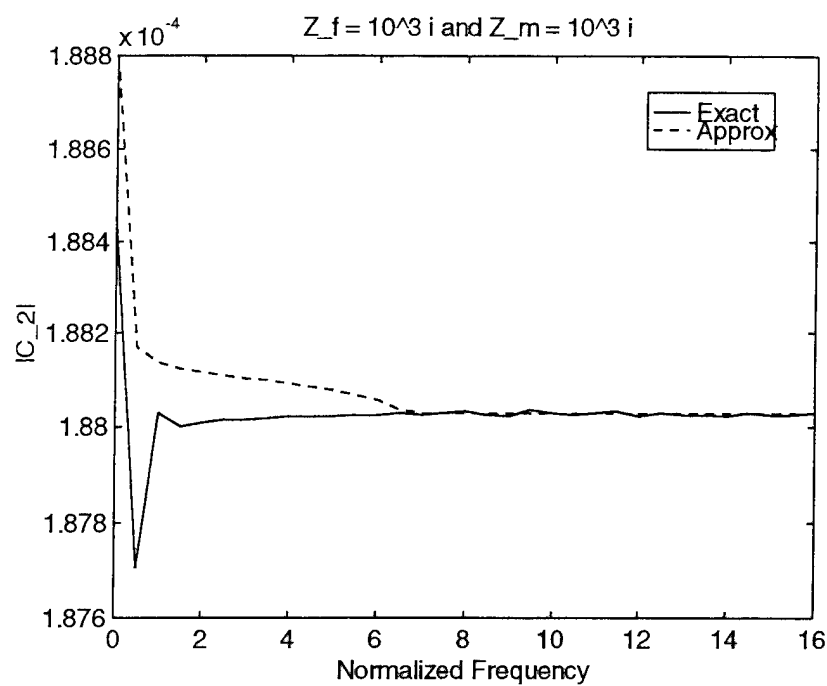Figure 4. Comparison for non-angular part of C_1 : Case 1

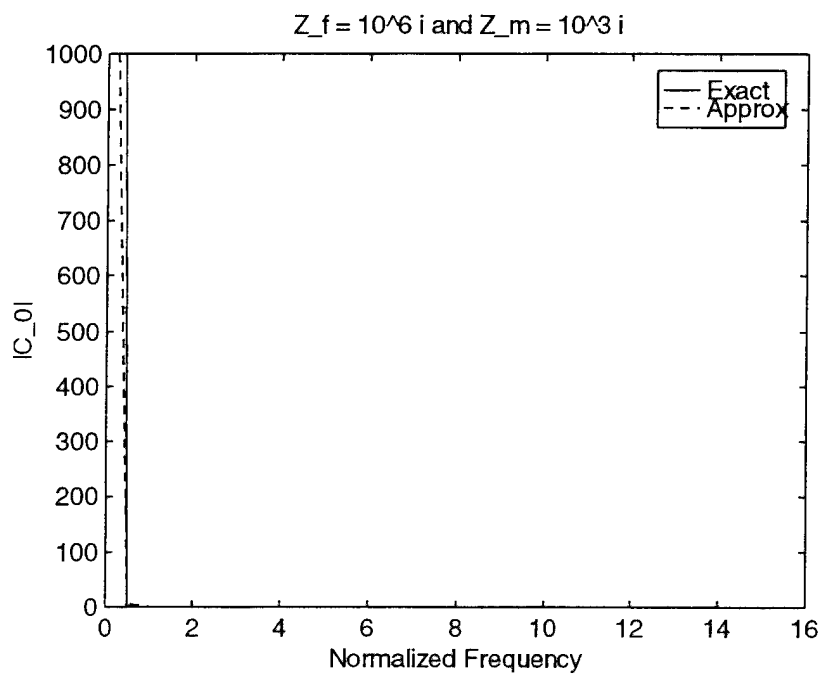Figure 5. Comparison for non-angular part of C_2: Case 1.

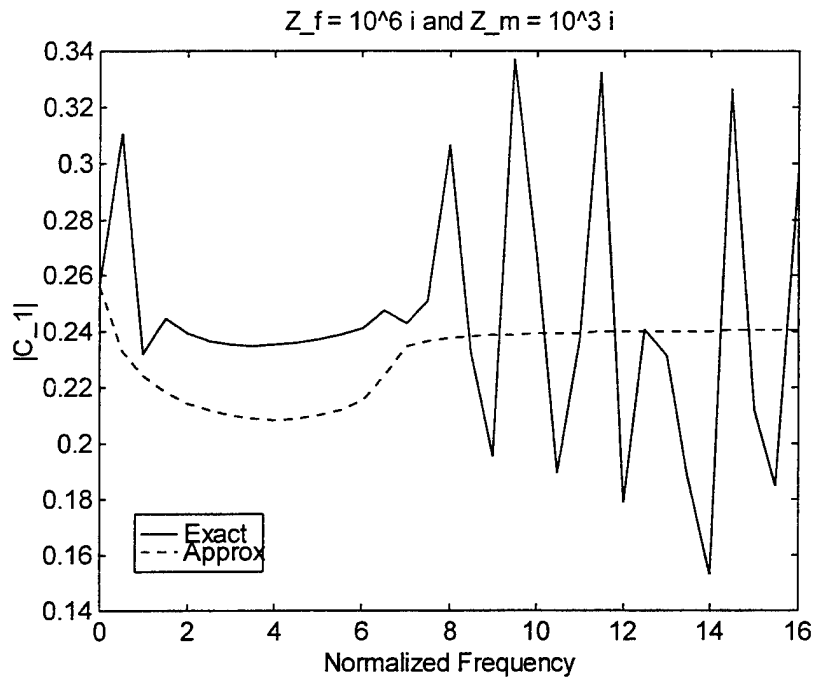Figure 6. Comparison for non-angular part of C_0: Case 2.
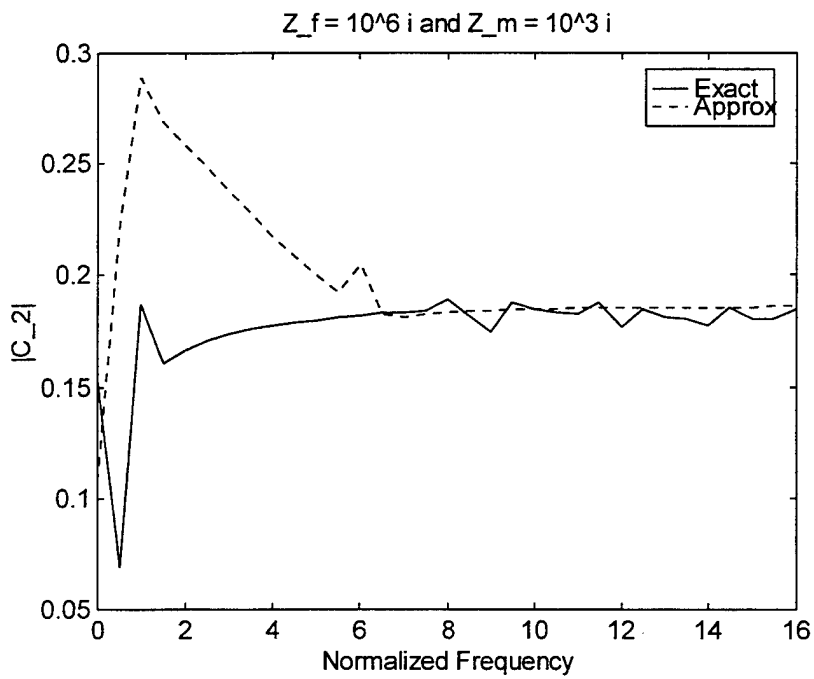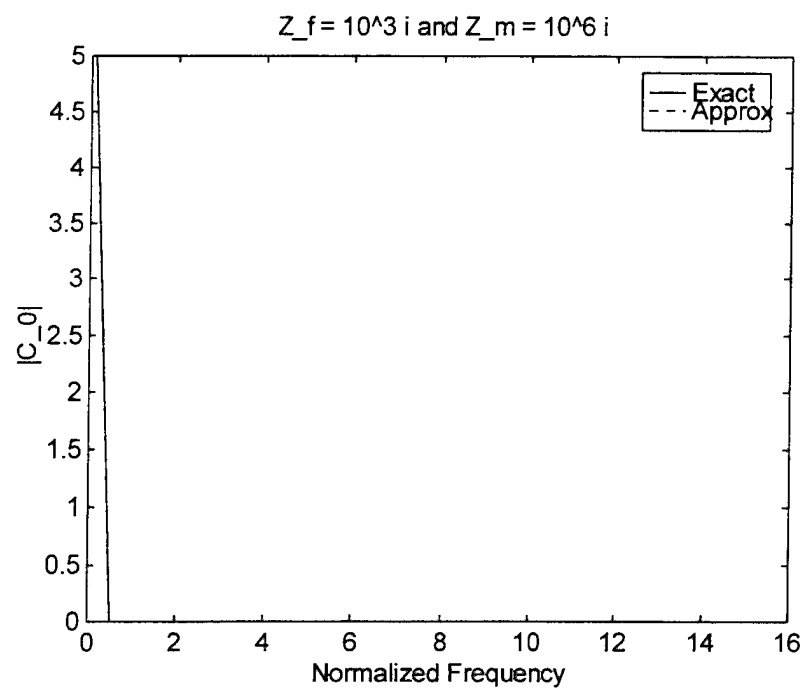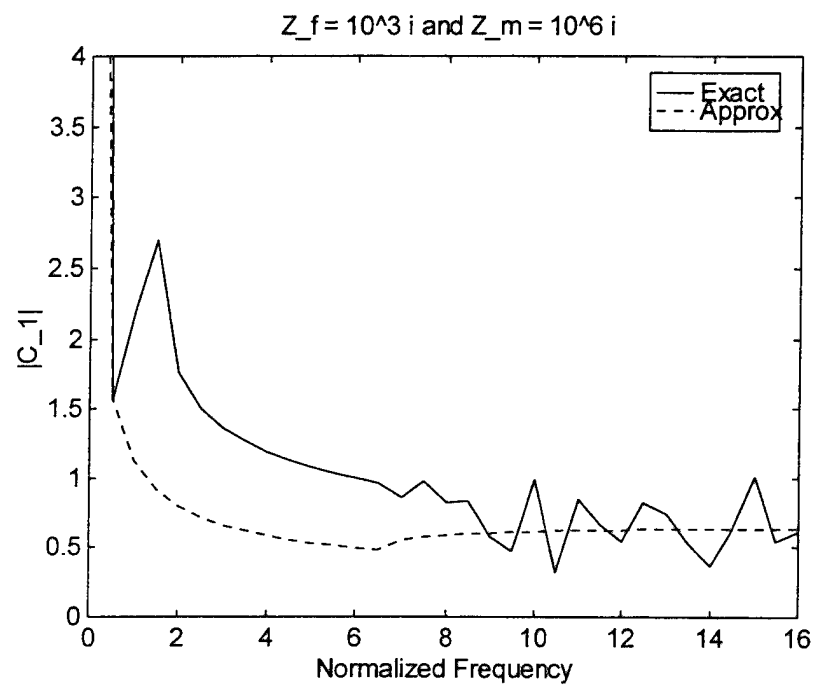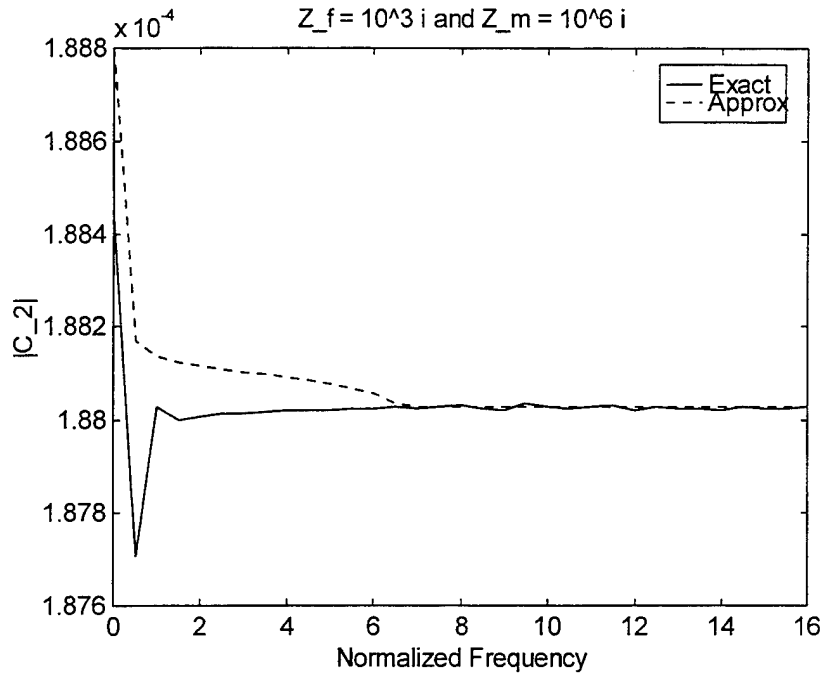
18

Figure 7. Comparison for non-angular part of C_1: Case 2.

Figure 8. Comparison for non-angular part of C_2: Case 2.

19

Figure 9. Comparison for non-angular part of C_0: Case 3.

Figure 10. Comparison for non-angular part of C_1: Case 3.

Figure 11. Comparison for non-angular part of C_2: Case 3.

REGIONS THAT MAY BE APPROXIMATED

Note that the scattering amplitude is significant only in a small region about the coincidence angle, θ_c, where

$$\sin \theta_c = \frac{1}{\sqrt{\Omega}} .$$

The width of this region decreases with increasing frequency. For most purposes, the amplitude can be treated as zero when more than 6 degrees from θ_c. In any case, the integral approximations are more than sufficient. Thus, numerical integration is only required in the immediate vicinity of θ_c.

SUMMARY

The frequency dependencies of target highlights have been examined. There are many areas where computational savings may be obtained, without loss of fidelity. Approximations, within tolerable errors, leading to further computational savings have been identified. These should allow a practical broadband simulation to be realized.

REFERENCES

Abramowitz, M. and I. A. Stegun. 1965. *Handbook of Mathematical Functions, with Formulas, Graphs, and Mathematical Tables*. Dover Publications, New York, NY.

Boersma, J. 1960. "Computation of Fresnel Integrals," *SIAM*, p.380.

Brekhovskikh, L. M. 1980. *Waves in Layered Media*, Academic Press, New York, NY.

Chabries, D. M. 1975. "High-Frequency Acoustic Scattering," NUC Technical Note 1522, Naval Undersea Center, San Diego, CA (Jun).

Gautschi, W. 1965. "Error Functions and Fresnel Integrals." In *Handbook of Mathematical Functions*, pp. 300–302, M. Abramowitz and I. A. Stegun, Eds., Dover Publications, New York, NY.

Gradshteyn, I. S. and I. M. Ryzhik. 1980. *Table of Integrals, Series, and Products*, p. 289, Academic Press, New York, NY.

Hayek, S. I. 1997. "A New Model for Scattering from a One Rib Reinforced Elastic Plate," ARL-PSU Memorandum (Mar), Applied Research Laboratory, Pennsylvania State University, State College, PA.

Hayek, S. I. and A. Karali. 1993. "Scattering of Sound Waves by Reinforced Panels," pp. 137–143, *Proceedings of Noise-93* (pp.137–143). 31 May 31–3 June, St. Petersburg, Russia.

Kouyoumjian, R. G. 1977. "The High-frequency Target Strength of Cone-shaped Scatterers, Part I: The Flat Back Cone," *ESL-OSU Technical Report 4720-1* (Aug), Electro-Sciences Laboratory, Ohio State University, Columbus, OH.

Lengua, G. A. 1991. "Specular Returns from a Foil-shaped Propeller with a Linear Pitch Variation," NOSC Technical Report 1489 (Nov), Naval Command, Control and Ocean Surveillance Center RDT&E Division[*], San Diego, CA.

Pauli, W. 1938. "On Asymptotic Series for Functions in the Theory of Diffraction of Light," *Physical Review*, vol. 54 (Dec), pp. 924–931.

Primakoff, H. and J.B. Keller. 1947. "Reflection and Transmission of Sound by Thin, Curved Shells," *Journal of the Acoustical Society of America*, vol. 19 (Sep), pp. 820–832.

Ruck, G. T., D.E. Barrick, W.D. Stuart, and C.K. Krichbaum. 1970. *Radar Cross-section Handbook*, Plenum Press, pp. 117–118. New York, NY.

Sides, D. J. 1976. "Echoes Formed by Multiple Reflections between Bulkheads and the Inner and Outer Hulls of a Submarine," SPEDAR (United Kingdom) Memorandum 154 (Nov).

Skudrzyk, E. J., S.I. Hayek, and A.D. Stuart. 1973. "Acoustic Diffractors, Part I—Plane Diffractors and Wedges," ARL-PSU Technical Memorandum 73-109 (May), Applied Research Laboratory-Pennsylvania State University, State College, PA.

---

[*] Formerly Naval Ocean Systems Center

REPORT DOCUMENTATION PAGE

Form Approved
OMB No. 0704-0188

1. AGENCY USE ONLY *(Leave blank)*	2. REPORT DATE August 1997	3. REPORT TYPE AND DATES COVERED Final

4. TITLE AND SUBTITLE

FREQUENCY DEPENDENCIES OF TARGET HIGHLIGHTS

6. AUTHOR(S)

G. A. Lengua

5. FUNDING NUMBERS

PE: 0602633N
AN: DN308047
WU: WT70

7. PERFORMING ORGANIZATION NAME(S) AND ADDRESS(ES)

Naval Command, Control and Ocean Surveillance Center (NCCOSC)
RDT&E Division (NRaD)
San Diego, California 92152–5001

8. PERFORMING ORGANIZATION REPORT NUMBER

TR 1752

9. SPONSORING/MONITORING AGENCY NAME(S) AND ADDRESS(ES)

Office of Naval Research
Applied Research Laboratory
800 North Quincy Street
Arlington, VA 22217–5660

10. SPONSORING/MONITORING AGENCY REPORT NUMBER

11. SUPPLEMENTARY NOTES

12a. DISTRIBUTION/AVAILABILITY STATEMENT

Approved for public release; distribution is unlimited.

12b. DISTRIBUTION CODE

13. ABSTRACT *(Maximum 200 words)*

The objective of this work was to examine the frequency dependencies of target highlights to determine where computational savings could be realized in broadband applications. Significant savings can be achieved by simply separating all frequency-independent calculations from the frequency loop. In some cases, highly accurate approximations will provide additional savings. In other cases, and contingent on the user's fidelity requirements, coarser approximations will yield yet more savings. Separation of frequency-independent factors and accurate approximations should be implemented as soon as feasible. Coarser approximations should be implemented, but their use should be contingent on a tolerance test.

14. SUBJECT TERMS

Mission area: Surveillance
acoustics
target models
broadband simulation

15. NUMBER OF PAGES

32

16. PRICE CODE

17. SECURITY CLASSIFICATION OF REPORT UNCLASSIFIED	18. SECURITY CLASSIFICATION OF THIS PAGE UNCLASSIFIED	19. SECURITY CLASSIFICATION OF ABSTRACT UNCLASSIFIED	20. LIMITATION OF ABSTRACT SAME AS REPORT

21a. NAME OF RESPONSIBLE INDIVIDUAL	21b. TELEPHONE *(include Area Code)*	21c. OFFICE SYMBOL
G. A. Lengua	(619) 553-1026 e-mail: lengua@nosc.mil	Code D711

INITIAL DISTRIBUTION